Synthesis and Properties of a New Metal-Rich Nickel Antimonide Telluride or Selenide: $Ni_{7-\delta}SbX_2$ ($\delta \approx 1.3$; X = Se or Te)

Thomas K. Reynolds, Joshua G. Bales, and Francis J. DiSalvo*

Department of Chemistry and Chemical Biology, Baker Laboratory, Cornell University, Ithaca, New York 14853

Received May 17, 2002. Revised Manuscript Received September 23, 2002

The two isotypic compounds $Ni_{5.66}SbTe_2$ and $Ni_{5.72}SbSe_2$ have been synthesized by high-temperature reaction of the elements or by using a flux method. They were both characterized by single-crystal X-ray diffraction. Both compounds crystallize in space group $I4/mmm$ with $Z = 2$. $Ni_{5.66}SbTe_2$ ($Ni_{5.72}SbSe_2$) has lattice parameters $a = b = 3.7824(5)$ Å and $c = 19.244(4)$ Å ($a = b = 3.7021(5)$ Å and $c = 18.593(3)$ Å). There is a high concentration of nickel vacancies (≈66%) on one of the three nickel sites (Wyckoff position 4e). Thermopower, thermal conductivity, resistivity, and magnetic susceptibility data for $Ni_{5.66}SbTe_2$ indicate nonmagnetic and metallic behavior.

1. Introduction

In the field of thermoelectrics, there are many guidelines for finding better thermoelectric materials. The dimensionless figure-of-merit ZT for a thermoelectric material is given by the equation $ZT = S^2T/\rho\kappa$ where S is the thermopower, T is the temperature, ρ is the electrical resistivity, and κ is the thermal conductivity. The larger this value is, the more efficient the material is for thermoelectric cooling and thermoelectric power generation.[1] At room temperature, the most efficient thermoelectric compound known to date is Bi_2Te_3; in commercial devices, solid solutions of Bi_2Te_3 and Sb_2Te_3 give the best device performance.[2−4] However, there are not many known ternary transition metal antimony tellurides or antimonide tellurides. The few examples include $AgSbTe_2$,[5] Mn_2SbTe,[6] $MnSb_2Te_4$,[7] $CdSb_2Te_4$,[8] Co_2SbTe,[9] $CoSbTe$,[10] $FeSbTe$,[10] $Nb_3Sb_2Te_5$,[11] $Cu_{9.1}TeSb_3$,[12] $ZrSb_2Te$,[13] Ni_2SbTe,[14] $PdSbTe$,[15] Pd_2SbTe,[16] and $Mo_3Sb_5Te_2$.[17] In many of these cases, the Sb and Te atoms are mixed on the same crystallographic site, and thus are not new structure types. There are also a few examples of transition metal antimony selenides or antimonide selenides. Among these are $AgSbSe_2$,[18] Zr_5Sb_3Se,[19] $FeSbSe$,[20] $CoSbSe$,[21] $CuSbSe_2$,[22] Cu_3SbSe_4,[23] $PdSbSe$,[15] $NiSbSe$,[15] $CrSbSe_3$[24], and $Ti_5Sb_{2.2}Se_{0.8}$.[25]

While searching for new thermoelectric materials in the Ni/Sb/Te system, we serendipitously prepared the nickel metal-rich antimonide telluride compound, $Ni_{5.66}SbTe_2$. It was originally grown from a K_3SbTe_3 flux. Reactive fluxes have been exploited to prepare novel compounds and to obtain small single crystals.[26,27] Usually the flux consists of a low melting binary alkali metal chalcogenide, and the alkali metal is incorporated into the structure. We sought to start with a ternary flux and gauge how well it works for synthesizing new compounds. K_3SbTe_3 was chosen because it melts congruently and is easy to prepare.[28]

The compound obtained from reacting K_3SbTe_3 with Ni contained no alkali metal and exhibited extensive nickel−nickel bonding. Also, there was a large percent-

* Corresponding author. Phone: 607-255-7238. Fax: 607-255-4137. E-mail: fjd3@cornell.edu.

(1) DiSalvo, F. J. *Science* **1999**, *285*, 703.
(2) Goldsmid, H. J. In *Thermoelectric Refrigeration*; Pion Ltd.: London, 1986; p 88.
(3) In *Encyclopedia of Materials Science Engineering*; Bever, M. B., Ed.; MIT Press: Cambridge, MA, 1986; p 4968.
(4) Scherrer, H.; Scherrer, S. In *CRC Handbook of Thermoelectrics*; Rowe, D. M., Ed.; CRC Press: Boca Raton, FL, 1995; p 211.
(5) Geller, S.; Wernick, J. H. *Acta Crystallogr.* **1959**, *12*, 46.
(6) Abdul Noor, S. S. *J. Appl. Phys.* **1987**, *61*, 3549.
(7) Azhdarova, D. S.; Rustamov, P. G.; Aliev, I. I.; Safarov, M. G. *Russ. J. Inorg. Chem.* **1982**, *27*, 909.
(8) Safarov, M. G.; Gamidov, R. S.; Poladov, P. M.; Bagirova, E. M. *Russ. J. Inorg. Chem.* **1991**, *36*, 899.
(9) Terzieff, P.; Ipser, H. *Monatsh. Chem.* **1992**, *123*, 35.
(10) Yamaguchi, G.; Shimada, M.; Koizumi, M. *J. Solid State Chem.* **1976**, *19*, 63.
(11) Jensen, P.; Kjekshus, A. *J. Less-Common Met.* **1967**, *13*, 357.
(12) Soetofte, I.; Makovicky, E.; Karup-Moller, S. *Z. Kristall.* **1998**, *213*, 382.
(13) Barthelat, J.-C.; Jeannin, Y.; Rancurel, J.-F. *C. R. Seances Acad. Sci., Ser. C* **1969**, *268C*, 1756.
(14) Makovetskii, G. I.; Shakhlevich, G. M. *Izv. Akad. Nauk SSSR, Neorg. Mater.* **1982**, *18*, 186.
(15) Foecker, A. J.; Jeitschko, W. *J. Solid State Chem.* **2001**, *162*, 69.
(16) Kim, W.-S.; Chao, G. Y. *Can. Mineral.* **1991**, *29*, 401.
(17) Dashjav, E.; Szczepenowska, A.; Kleinke, H. *J. Mater. Chem.* **2002**, *12*, 345.
(18) Schanow, W.; Range, K.-J. *Mater. Res. Bull.* **1983**, *18*, 39.
(19) Garcia, E.; Corbett, J. D. *Inorg. Chem.* **1990**, *29*, 3274.
(20) Hahn, H.; Klingen, W. *Naturwissenschaften* **1965**, *52*, 494.
(21) Nahigian, H.; Steger, J.; McKinzie, H. L.; Arnott, R. J.; Wold, A. *Inorg. Chem.* **1974**, *13*, 1498.
(22) Imamov, R. M.; Pinsker, Z. G.; Ivcen, A. I. *Kristallografiya* **1964**, *9*, 853.
(23) Pfitzner, A. *Z. Kristall.* **1994**, *209*, 685.
(24) Odink, D. A.; Carteaux, V.; Payen, C.; Ouvrard, G. *Chem. Mater.* **1993**, *5*, 237.
(25) Kleinke, H. *J. Alloys Compd.* **2002**, *336*, 132.
(26) Sunshine, S. A.; Kang, D.; Ibers, J. A. *J. Am. Chem. Soc.* **1987**, *109*, 6202.
(27) Kanatzidis, M. G.; Sutorik, A. *Prog. Inorg. Chem.* **1995**, *43*, 151.
(28) Jung, J. S.; Wu, B.; Stevens, E. D.; O'Connor, C. J. *J. Solid State Chem.* **1991**, *94*, 362.

10.1021/cm020585r CCC: $22.00
Published on Web 10/31/2002

age of vacancies at one of the nickel sites. Because of the large amount of metal−metal bonding, we decided to investigate the magnetic and electrical transport properties of the compound. The analogous selenide compound could also be prepared from a stoichiometric mixture of the elements. However, in that case, the compound could not be prepared phase pure. Hence, only crystal structure data for the selenide compound will be presented in this paper.

2. Experimental Section

Reagents. All reagents were used as received: nickel powder, 99.9% purity, Strem Chemicals, Inc., Newburyport, MA; tellurium powder, 99.99% purity, −30 mesh, Cerac, Inc., Milwaukee, WI; selenium pellets, 99.9999% purity, Atomergic Chemetals Corp., Plainview, NY; antimony shot, 99.999% purity, Cerac; potassium chunk, cylindrical, >98% purity, Fluka Chemical Corp., Ronkonkoma, NY.

Synthesis. K_2Te. Potassium telluride was synthesized from the stoichiometric combination of the elements in liquid ammonia, in a manner similar to other literature preparations of alkali metal chalcogenides.[29]

K_3SbTe_3. Potassium antimony telluride was synthesized from the stoichiometric reaction of K_2Te, Sb, and Te at elevated temperatures.[28] K_2Te, Sb, and Te were ground together in an argon-filled glovebox. They were subsequently loaded into a carbon-coated quartz tube and heated to 550 °C over 6 h. The mixture was then held at this temperature for 6 h, and then cooled over 28 h to room temperature. The air-sensitive reddish-black powder was then ground up and stored in an argon-filled glovebox for later use. Powder X-ray diffraction revealed a phase pure sample (Scintag XDS 2000, Cu Kα radiation).

$Ni_{5.66}SbTe_2$. Nickel antimonide telluride was originally isolated from the reaction of Ni metal and K_3SbTe_3 in a 3:1 ratio. The starting materials were placed in a carbon-coated quartz tube and heated to 700 °C over 7 h. The furnace was then held at this temperature for 100 hours, and then slowly cooled to room temperature over another 100 hours. The product consisted mainly of a powder containing K_2Te, Sb_2Te_3, and K_3SbTe_3. From this powdery matrix, a few black, irregular blocklike crystals of $Ni_{5.66}SbTe_2$ could be isolated. Subsequently, the compound could be prepared in bulk from the stoichiometric reaction of the elements. Ni, Sb, and Te were combined stoichiometrically in a quartz tube and heated to 900 °C over 9 h. The mixture was then held at this temperature for 100 hours and then slow-cooled to room temperature over another 100 hours. The resultant powder was then ground up, pressed into a pellet, and sealed in a quartz tube. After the pellet was annealed for 100 hours at 900 °C, the powder X-ray diffraction pattern showed phase-pure product. Attempts to grow the stoichiometric version of the compound, Ni_7SbTe_2, yielded $Ni_{5.66}SbTe_2$ and excess free nickel in the sample. This ternary compound is stable in air.

$Ni_{5.72}SbSe_2$. Nickel antimonide selenide was prepared from a mixture of the elements in a ratio 7:1:2 Ni/Sb/Se. Ni, Sb, and Se were combined in a quartz tube and heated to 900 °C, and then held at this temperature for 100 hours. The reaction products were subsequently cooled to room temperature over 100 hours. This yielded a large number of black, flat, platelike crystals growing from a polycrystalline mass. As in the case of the telluride compound, the structure solution led to a partial occupancy on one of the Ni sites. Unfortunately, this compound could not be prepared phase pure. There was always a large amount of Ni_3Se_2 present, as evidenced in the powder diffraction patterns of the polycrystalline mass. Hence, the physical and magnetic properties of this compound were not determined. This compound is also stable in air.

Transport Property Measurements. The electrical resistivity of the telluride was measured in a home-built apparatus using a standard 4-probe AC technique.[30] Annealed pressed pellets (900 °C) of the compound were cut with a diamond saw into a bar which measured 3.9 mm × 3.6 mm × 6.0 mm. Current contacts to the sample were made with 0.05-mm-thick copper foil which was attached to the end faces of the bar with indium solder. The voltage leads were made with 38 AWG copper wires by use of silver epoxy (H20E, EpoTek) and attached to a flat face on the bar. To do variable temperature measurements, the probe was designed to fit into a standard-size helium dewar. The frequency of the current signal was set to 23 Hz. Data were taken at set time intervals as the temperature was lowered at a rate of ≤ 1.5 K/min. Because of uncertainties in measuring the cross-sectional area and voltage lead contact spacing, a ±10% error in absolute value of the resistivity is assumed.[30]

Thermopower and thermal conductivity were measured simultaneously on a home-built apparatus using a steady-state technique.[30] The same bar-shaped sample used in the resistivity measurements was used in this measurement. Both ends of the sample were wet with indium metal in order to ensure good thermal and electrical contact between the sample and the thermocouples. A 40 AWG Au,Fe(0.07%)/Chromel-*p* thermocouple was attached to each end of the sample. On one end of the sample, a 6 kΩ resistor was attached in order to serve as a resistive heater. The other end of the sample was attached to a removable copper screw which served as the sample mount base and heat sink. To obtain reliable thermal conductivity measurements, a good vacuum around the sample was needed. Using standards of thermal conductivity, we showed that the pressure attained, 5×10^{-6} Torr, is sufficient to remove heat losses through the gas. A copper radiation shield around the sample served to reduce radiative heat loss which could affect the thermal conductivity measurements. By sequentially and slowly lowering the probe inside a helium dewar, different sample temperatures could be achieved. When the probe reached a stable temperature inside the dewar, voltage (V) measurements were made by varying the temperature gradient across the sample. Typically, the maximum temperature differential (ΔT) used was 1.5 K. By finding the slope of V vs ΔT, the thermopower could be obtained. Because sample voltage was measured from the chromel-*p* wires, a correction for their contribution to the thermopower was applied. At each ΔT, the power to the resistor (P) was also measured. From the slope of P vs ΔT, and subsequent correction with the geometric factor (A/l), the thermal conductivity was obtained. The accuracy of the thermopower measurements is estimated to be ±5% as estimated from standards, while the accuracy of the thermal conductivity values is estimated to be ±15%.[30]

Magnetic Property Measurements. Magnetic susceptibility data were collected on a Quantum Design SQUID magnetometer. Samples cut from the same pellet used for transport property measurements were loaded into gelatin capsules for the measurement (typically 0.25 g). Data were obtained in the DC mode with fields between 1000 Oe and 20 000 Oe. Afterward, a correction for the diamagnetic susceptibility of the gelatin capsule was applied to the data.

Electron Microscopy. Electron microprobe analysis was carried out on a JEOL 8900R electron microprobe. The accelerating voltage was set to 15 kV and the probe current was typically set to 5−10 nA. Energy dispersive spectroscopy (EDS) was carried out on flat faces of single crystals. Collection time was typically 30 s. Because K, Sb, and Te all have overlapping lines in the EDS spectra, wavelength dispersive spectroscopy (WDS) was also used to determine the presence or absence of certain elements. The possibility of inclusion of K in the crystal was eliminated when WDS failed to show any peaks for K, and revealed the presence of only Ni, Sb, and Te. Semiquantitative EDS analysis yielded the ratio of the ele-

(29) Klemm, W.; Sodomann, H.; Langmesser, P. *Z. Anorg. Allg. Chem.* **1939**, *241*, 281.

(30) Jones, C. D. W.; Regan, K. A.; DiSalvo, F. J. *Phys. Rev. B: Condens. Matter Mater. Phys.* **1998**, *58*, 16057.

Table 1. Crystal Data and Structure Refinement of $Ni_{5.66}SbTe_2$ and $Ni_{5.72}SbSe_2$

empirical formula	$Ni_{5.66}SbTe_2$	$Ni_{5.72}SbSe_2$
formula weight	709.25	615.49
temperature	164(2) K	293(2) K
wavelength	0.71073 Å	0.71073 Å
space group	*I*4/*mmm* (no. 139)	*I*4/*mmm* (no. 139)
unit cell dimensions	$a = 3.7824(5)$ Å	$a = 3.7021(5)$ Å
	$c = 19.244(4)$ Å	$c = 18.593(4)$ Å
volume	275.32(8) Å^3	254.83(7) Å^3
Z	2	2
density (calculated)	8.556 mg/m^3	8.021 mg/m^3
absorption coefficient	34.0 mm^{-1}	40.0 mm^{-1}
F(000)	627	558
crystal color	black	black
crystal size	0.1 × 0.1 × 0.08 mm^3	0.41 × 0.23 × 0.02 mm^3
θ range for data collection	4.24 to 30.42°	4.38 to 29.12°
index ranges	$-5 \le h \le 5$, $-5 \le k \le 5$, $-26 \le l \le 26$	$-5 \le h \le 5$, $-5 \le k \le 5$, $-24 \le l \le 24$
reflections collected	1703	1433
independent reflections	159 [R(int) = 0.0320]	132 [R(int) = 0.1701]
absorption correction	empirical	empirical
refinement method	full-matrix least-squares on F^2	full-matrix least-squares on F^2
data/restraints/parameters	159/0/17	132/0/17
goodness-of-fit on F^2	1.052	1.279
final R indices [$I>2\sigma(I)$][a,b]	$R_1 = 0.0225$, $wR_2 = 0.0537$	$R_1 = 0.0534$, $wR_2 = 0.1199$
R indices (all data)	$R_1 = 0.0229$, $wR_2 = 0.0541$	$R_1 = 0.0534$, $wR_2 = 0.1199$
extinction coefficient	0.0248(14)	0.010(2)
largest diff. peak and hole	1.069 and −3.461 eÅ^{-3}	1.995 and −2.568 eÅ^{-3}
weighting scheme	$w^{-1} = [\sigma^2(F_o2) + (0.0340P)^2 + 5.3532P]$ where $P = [\max(F_o2,0) + 2F_c2]/3$	$w^{-1} = [\sigma^2(F_o2) + (0.0132P)^2 + 15.7927P]$ where $P = [\max(F_o2,0) + 2F_c2]/3$

[a] $R_1 = \Sigma||F_o| - |F_c||/\Sigma|F_o|$. [b] $wR_2 = [\Sigma w(F_o2 - F_c2)^2/\Sigma w(F_o2)^2]^{1/2}$.

ments Ni/Sb/Te as 5.36:1:1.82. However, considering Sb and Te have a very large amount of overlap in the EDS spectrum, the latter ratio may not be very accurate. The ratio of Ni/(Sb+Te), however, is 5.71:3, which is close to that obtained from the crystal structure solution which gives a Ni/(Sb+Te) ratio of 5.66:3.

For $Ni_{5.72}SbSe_2$, under similar microprobe conditions, EDS yielded a ratio of 5.77:1:1.87 for Ni/Sb/Se. Again, this agrees reasonably well with the crystal structure solution.

Crystallographic Study. For the telluride compound, a small, black, irregular blocklike crystal with approximate dimensions 0.1 mm × 0.1 mm × 0.08 mm was isolated from the reaction products under a microscope. The crystal was then mounted in poly(butenes) (viscosity at 99 °C 109−125 cst, d 0.88−0.89, catalog no. 38,868-8, Aldrich) for data collection at 164 K. The instrument used to collect single-crystal data was a Bruker SMART CCD diffractometer equipped with a 1 K CCD detector and a 3 kW molybdenum sealed-tube X-ray generator. Data were collected with the program SMART.[31] Three different ω scans (ϕ = 0°, 120°, and 240°) were performed with a $\Delta\omega = 0.3°$ and an exposure time of 20 s. Finally, a ϕ scan was taken with $\Delta\phi = 0.3°$ and an exposure time of 20 s. The refinement of the unit cell took place during the integration of the data using SAINT and was based on the strong reflections.[31] Space group determination was done in the program XPREP from the SHELXTL program suite.[32] Subsequent structure solution and refinement were done with the two programs SIR92 and SHELXL-97.[32,33] Because the crystal was somewhat irregular, it was difficult to apply an analytical face-indexed absorption correction, and thus an empirical absorption correction based on SADABS was applied.[34] A PSI-scan absorption correction was also used but it did not improve the refinement.

For $Ni_{5.72}SbSe_2$, a flat plate of dimensions 0.41 mm × 0.23 mm × 0.02 mm was selected. The crystal was fixed to the end of a very thin silica fiber with epoxy. Data for this crystal were collected at room temperature. The data collection used the same profile as that for the telluride compound, and an absorption correction based on equivalents using X-Shape was applied to the data.[35]

Crystal structure refinement data can be found in Table 1. The atomic coordinates, as well as U(eq), can be found in Tables 2 and 3.

Table 2. Atomic Coordinates and Equivalent Isotropic Displacement Parameters (Å^2 × 10^3) for $Ni_{5.66}SbTe_2$; *U*(eq) Is Defined as One-Third of the Trace of the Orthogonalized U_{ij} Tensor

	Wyckoff position	*x*	*y*	*z*	*U*(eq)
Ni(1)	2a	0	0	0	3.4(4)
Ni(2)	8g	0	1/2	0.0937(1)	4.1(3)
Ni(3)[a]	4e	0	0	0.3098(2)	5.7(14)
Sb	2b	0	0	1/2	2.9(3)
Te	4e	0	0	0.1814(1)	4.3(3)

[a] Ni(3): 0.330(8) occupation.

Table 3. Atomic Coordinates and Equivalent Isotropic Displacement Parameters (Å^2 × 10^3) for $Ni_{5.72}SbSe_2$; *U*(eq) Is Defined as One-Third of the Trace of the Orthogonalized U_{ij} Tensor

	Wyckoff position	*x*	*y*	*z*	*U*(eq)
Ni(1)	2a	0	0	0	15.8(10)
Ni(2)	8g	0	1/2	0.1001(1)	16.3(8)
Ni(3)[a]	4e	0	0	0.3020(6)	22(3)
Sb	2b	0	0	1/2	15.0(8)
Se	4e	0	0	0.1810(2)	15.9(8)

[a] Ni(3): 0.359(17) occupation.

Structure Solution of $Ni_{5.66}SbTe_2$. The space group for the compound was determined using the program XPREP. The best choice of space group was *I*4/*mmm*. The initial structure solution from SIR92 yielded the position of 2 Ni atoms, and 2

(31) SMART and SAINT: Data Collection and Processing Software for the SMART System; Bruker AXS, Inc.: Madison, WI, 1995.

(32) Sheldrick, G. M. SHELXTL Version 5.1; Bruker AXS, Inc.: Madison, WI, 1996.

(33) Altomare, A.; Cascarano, G.; Giacovazzo, C.; Guagliardi, A. J. *J. Appl. Crystallogr.* **1993**, *26*, 343.

(34) Sheldrick, G. M. The computer program SADABS is used by Bruker CCD diffractometers; Institut für Anorganische Chemie der Universität Göttingen: 1996.

(35) STOE X-Shape Version 1.01 − Program for Crystal Optimization for Numerical Absorption Correction; STOE and Cie GmbH: Darmstadt, 1996.

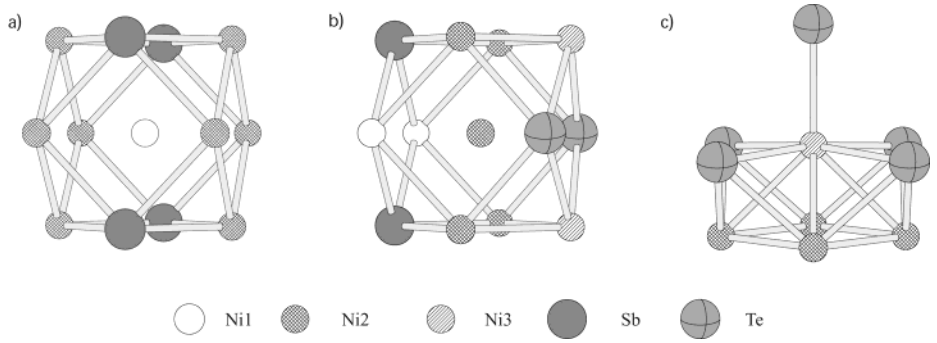

Figure 1. Local coordination environments around the three distinct nickel sites: (a) Ni1, (b) Ni2, and (c) Ni3.

atoms that were either Te atoms or Sb atoms. Because Te and Sb differ in atomic number by only one, distinction between the two by X-ray crystallography alone is difficult, if not impossible. This initial solution, when refined with SHELXL-97, had an R_1 of 12.99% and a wR_2 of 39.87%. The difference Fourier map had only one outstanding peak which corresponded to a Ni atom. After refining with this new Ni atom, R_1 dropped to 11.70% and wR_2 to 38.38%. At this point, SHELXL-97 warned that an extinction correction needed to be applied. On the next cycle of refinement, this yielded an R_1 of 8.70% and a wR_2 of 36.06%. At this point, there were no features in the difference Fourier map which could correspond to any new atoms. On the basis of the microprobe data which yielded an approximate ratio of Sb/Te of 1:2, and the fact that in the known compound, $Ni_{2.86}Te_2$,[36] a similar bonding environment is seen for Te, it was decided that one of the atoms being refined as Te, was actually Sb. The site multiplicities corresponded to a 1:2 ratio Sb/Te. On the next cycle of refinement, R_1 dropped to 8.68% and wR_2 dropped to 35.13%. At this point, the displacement factor of 1 of the Ni atoms was extremely high. Occupancy of this site was then refined, and the thermal factor came to a reasonable value. R_1 dropped significantly to 2.82%, and wR_2 dropped to 11.51%. A similar vacancy occurs in the known compound $Ni_{2.86}Te_2$.[36] The Fourier difference map was essentially featureless at this point. After refining anisotropically, the final R_1 was 2.25%, and the wR_2 was 5.42%. The residual electron density had a maximum of 1.07 eÅ^{-3} near Ni2 (1.22 Å) and a minimum of −3.46 eÅ^{-3} near Te1 (0.56 Å). Electron density differences found next to elements with large Z are usually ascribed to data truncation; here $2\theta < 61°$. The final formula was $Ni_{5.66}SbTe_2$, which corresponds well with microprobe data. No new symmetries were suggested by the program ADDSYM in the Platon Package.[37,38] STRUCTURE TIDY was used to standardize the coordinate positions of the atoms.[39]

Structure Solution of $Ni_{5.72}SbSe_2$. A crystal structure solution pathway similar to that of the telluride compound yielded a final solution of the isostructural selenide compound. In this case, it was easy to distinguish the Se from the Sb because of the large difference in atomic number between the two atoms.

3. Results and Discussion

Structure Description. The structure of $Ni_{5.66}SbTe_2$ consists of a 3-dimensional framework dominated by nickel−nickel interactions. There are 5 crystallographically distinct atomic sites, 3 of which belong to Ni. Ni1, Ni2, and Sb1 all have cuboctahedral bonding environments. Ni1 forms a distorted cuboctahedron with 8 bonds to Ni2 at 2.61 Å, and 4 bonds to Sb1 at 2.67 Å (Figure 1a). Ni2 forms another distorted cuboctahedron with 2 bonds to Te1 at 2.53 Å, 2 bonds to Ni1 and Sb1 at 2.61 Å, 2 bonds to Ni3 at 2.65 Å, and 4 bonds to it's symmetrically related equivalents at 2.67 Å (Figure 1b). Sb1 has 8 Ni2 at 2.61 Å, and 4 Ni1 at 2.67 Å, thus forming another distorted cubotahedron. All Ni−Ni distances are larger than that found in Ni metal (2.49 Å), but well within bonding distance (a van der Waals contact would be 3.26 Å). Ni3 and Te1, on the other hand, have irregular coordination environments. Ni3 is above the center of a square plane of Te1 atoms, each at 2.68 Å. Below this square plane of Te1 atoms, there is another square plane of Ni2 atoms at 2.65 Å, rotated 45° with respect to the plane of Te1 atoms (Figure 1c). The final atom in the coordination environment of Ni3 is a capping Te1 atom at 2.47 Å. Thus, the coordination number for Ni3 is 9 (4 Ni atoms, 5 Te atoms). The Ni3 site is only partially occupied (near $^1/_3$ occupation). This is not unprecedented, however, because in the compound $Ni_{2.86}Te_2$,[36] a similar situation exists. In this compound, a partially occupied Ni site also has the same type of coordination environment as the Ni3 atom in $Ni_{5.66}SbTe_2$. Te1 has an environment similar to that of Ni3. There are 4 Ni3 atoms at 2.68 Å which form a square plane around the Te1 atom. In this case, the Te1 atom is below this square plane of Ni3 atoms. There is another square plane of Ni2 atoms at 2.53 Å, rotated 45° with respect to the other square plane of Ni atoms. The final atom in the coordination environment of Te1 is another Ni3 atom above the square plane of Ni3 atoms, and at 2.47 Å. The connectivity of the structure is apparent when viewed perpendicular to the a-axis. The structure consists of a NaCl-type (100) plane of NiSb stoichiometry. This plane is sandwiched between two planar Ni layers, where Ni again adopts a square planar arrangement in each layer. The Ni density in these layers is twice that of the NiSb layer, and the Ni−Ni distance in the Ni layers is smaller by $\sqrt{2}$ than that in the NiSb layers. These three layers are further sandwiched between two NiTe layers, which also are NaCl-type (100) planes. The layers then repeat in a staggered fashion to give a body centered unit cell. Concentrating on only Ni−Ni interactions, one sees that 2-dimensional slabs are created, with connectivity between the slabs established through Ni−Te bonds (Figure 2a). A unit cell representation is shown in Figure 2b. $Ni_{5.72}SbSe_2$ is isostructural to the telluride compound. Within $\pm 2\sigma$, the stoichiometries determined by the refinement are the same.

(36) Kok, R. B.; Wiegers, G. A.; Jellinek, F. *Recueil des Travaux Chimiques des Pays-Bas et de la Belgique* **1965**, *84*, 1585.
(37) Spek, A. L. *J. Appl. Crystallogr.* **1988**, *21*, 578.
(38) Spek, A. L. *Acta Crystallogr.* **1990**, *A46*, C34.
(39) Gelato, L.; Parthé, E. STRUCTURE TIDY program, PC Version; University of Geneva: Switzerland, 1992.

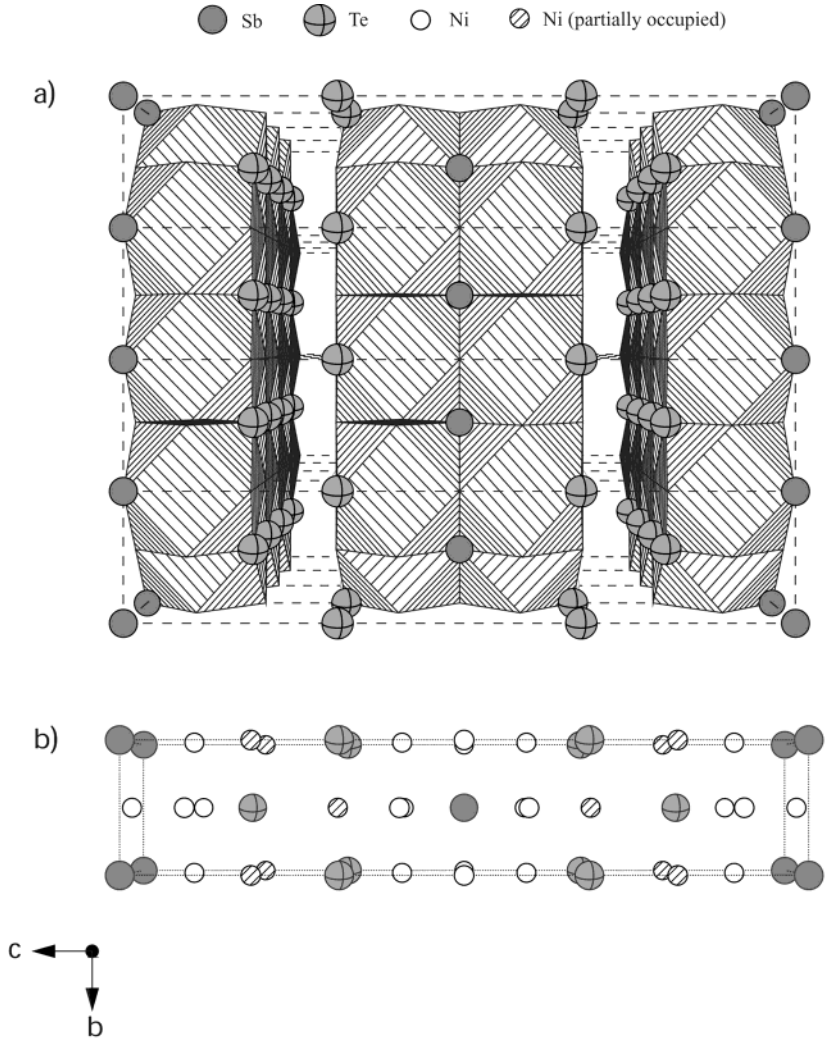

Figure 2. (a) View down the *a*-axis, showing the polyhedral slabs. Ni metal atoms are not shown for clarity. (b) View of a single unit cell, showing the positions of the partially occupied Ni3 sites.

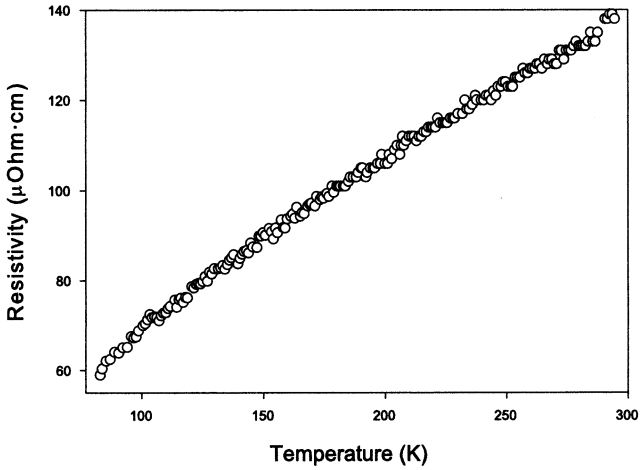

Figure 3. Electrical resistivity vs temperature for an annealed polycrystalline bar of $Ni_{5.66}SbTe_2$.

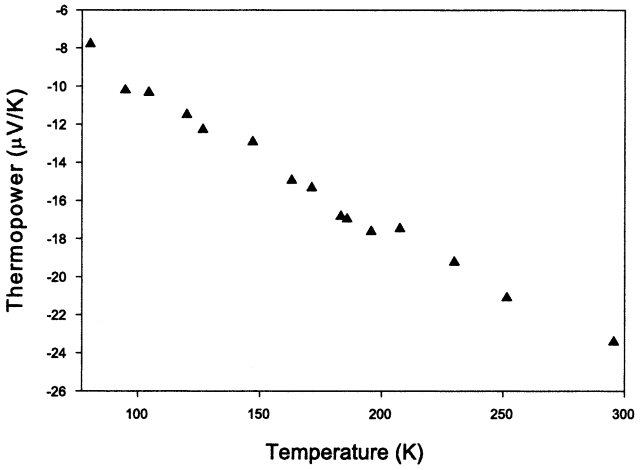

Figure 4. Thermopower vs temperature for an annealed polycrystalline bar of $Ni_{5.66}SbTe_2$.

Transport Properties. Because there is significant Ni−Ni bonding within the structure, metallic characteristics are expected. The electrical resistivity decreases from 140 $\mu\Omega$·cm at 295 K to 60 $\mu\Omega$·cm at 80 K (Figure 3). This decrease in resistivity with decreasing temperature, along with the typical values observed for a "dirty" metal, is indicative of metallic behavior.

The thermopower was measured from 298 to 80 K. The value of the thermopower continually decreases in magnitude from −24 to −8 μV/K in this temperature regime (Figure 4). These small values for thermopower are also indicative of metallic behavior, and the negative sign indicates that electrons are the dominant charge carrier in the material. These thermopower values are

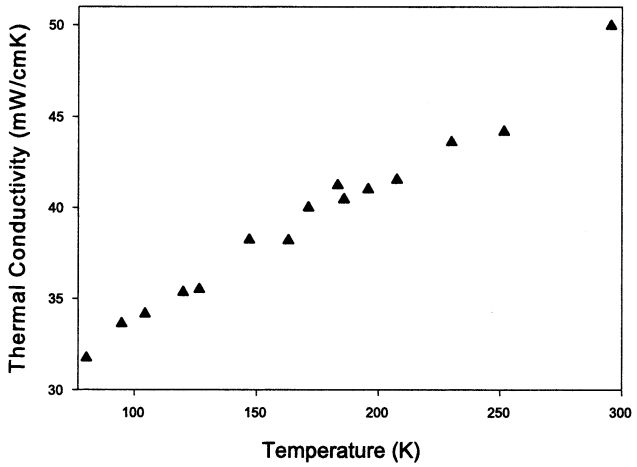

Figure 5. Thermal conductivity vs temperature for an annealed polycrystalline bar of $Ni_{5.66}SbTe_2$.

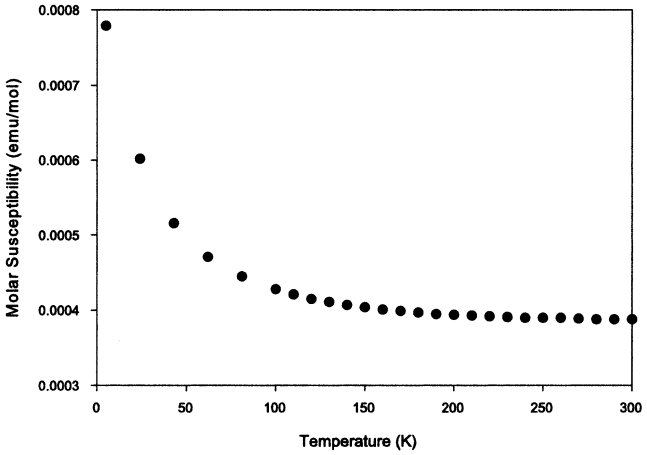

Figure 6. Molar magnetic susceptibility of polycrystalline $Ni_{5.66}SbTe_2$ from room temperature to 6 K.

much smaller than would be needed in a good thermoelectric material.

The thermal conductivity of this compound is fairly low for a metal. The values decrease from 50 mW/cm·K at 298 K to 32 mW/cm·K at 80 K (Figure 5). This behavior is likely caused by the large number of vacancies on the Ni3 site and the presence of heavy anions. In simple metals, the thermal conductivity generally increases on cooling from room temperature. A calculation of the Wiedemann−Franz product, $\rho\kappa = LT$, gives $L = 2.26 \times 10^{-8} \pm 5\%$ W·Ω/K^2, independent of T. In metals we expect $L = L_0 = 2.45 \times 10^{-8}$ W·Ω/K^2. Thus, $L/L_0 \approx 1$ indicating that the conduction electrons rather than phonons are the dominant carriers of heat in the compound. A decrease in thermal conductivity with temperature is also observed in metallic glasses and some alloys, which also obey the Wiedemann−Franz law.[40]

Because there is a prevalence of Ni−Ni bonding, we also investigated the magnetic properties of the material down to 6 K. Interesting magnetic phenomena can often occur when there are metal−metal interactions. As can be seen in Figure 6, the molar susceptibility is temperature independent at high temperatures, and then starts to increase rapidly at low temperatures ($T < 100$ K). This "Curie tail" is often observed when paramagnetic impurities are present in the sample. The data were fit to the Curie−Weiss law, $\chi = \chi_0 + C/(T - \Theta)$, where χ is the total magnetic susceptibility, χ_0 is the temperature independent magnetic susceptibility, C is the Curie constant, T is the temperature, and Θ is the Curie−Weiss constant. A fit to the data from 20 to 300 K gives a temperature-independent Pauli paramagnetic susceptibility, χ_0, of 3.50×10^{-4} emu/mol, a Curie constant of 9.34×10^{-3} emu/mol·K, and a Curie−Weiss constant of −16.45 K. In that case, an impurity concentration of 0.04% is calculated from the Curie constant and is consistent with the reported Ni purity (99.9%). Considering Fe is the most common impurity, we assume the paramagnetic impurity is Fe with a moment of 4.9 μ_B per Fe atom ($g = 2$, $S = 2$).

Conclusions

A new compound $Ni_{5.66}SbTe_2$ and it's isostructural analogue $Ni_{5.72}SbSe_2$ have been synthesized. These compounds could be synthesized only with a partial occupation of one of the Ni sites. $Ni_{5.66}SbTe_2$ exhibits typical metallic behavior with high conductivity and low thermopower. It has fairly low thermal conductivity for a metal, which may result from the high Ni vacancy concentration. It exhibits temperature-independent Pauli paramagnetism, which is also typical for a metal. Although this compound is a poor candidate for a thermoelectric cooling material, there are other areas in which this compound may be useful. Binary nickel antimonide, Ni_3Sb, has the fastest self-diffusion ever observed in a metallic system,[41] and this compound might also exhibit similar fast ion conductivity. In Ni_3Sb, the unusually high vacancy concentration on one of the nickel sites accounts for its fast mobility.[42]

Acknowledgment. This work was funded by NSF grant DMR-0115732. We thank Dr. Emil B. Lobkovsky for assistance with single crystal data collection. We also thank John Hunt for guidance in using the electron microprobe facility in the Cornell Center for Materials Research which is supported through a MRSEC grant (DMR-0079992). We also thank the American Society for Engineering Education for support through a National Defense Science and Engineering Graduate Fellowship (NDSEG).

Supporting Information Available: X-ray crystallographic file for the two titled compounds (CIF). This material is available free of charge via the Internet at http://pubs.acs.org.

CM020585R

(40) Choy, C. L.; Leung, W. P.; Ng, Y. K. *J. Appl. Phys.* **1989**, *66*, 5335.

(41) Bester, G.; Meyer, B.; Fähnle, M. *Phys. Rev. B: Condens. Matter Mater. Phys.* **1998**, *57*, R11 019.

(42) Randl, O. G.; Vogl, G.; Kaisermayr, M.; Bührer, W.; Pannetier, J.; Petry, W. *J. Phys.: Condens. Matter* **1996**, *8*, 7689.